Joule

CellPress

Article

Climatic Impacts of Wind Power

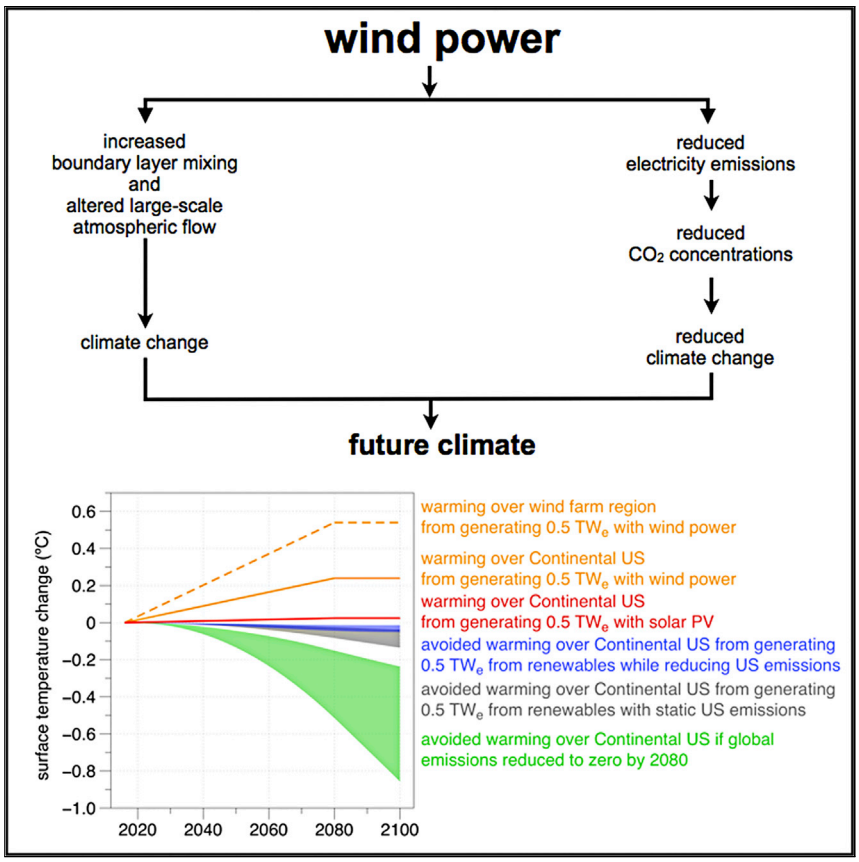

Wind beats fossil, but wind power does cause non-negligible climatic impacts. This study advances work on wind power's climate impacts by: (1) providing a mechanistic explanation for wind turbines' climate impacts by comparing numerical simulations with observations, (2) filling a current gap between small- and very-large-scale wind power simulation studies, (3) making the first quantitative comparison between wind power's climatic impacts and benefits, and (4) using the same framework to make a quantitative comparison with solar power.

Lee M. Miller, David W. Keith

lmiller@seas.harvard.edu (L.M.M.)
david_keith@harvard.edu (D.W.K.)

HIGHLIGHTS

Wind power reduces emissions while causing climatic impacts such as warmer temperatures

Warming effect strongest at night when temperatures increase with height

Nighttime warming effect observed at 28 operational US wind farms

Wind's warming can exceed avoided warming from reduced emissions for a century

Miller & Keith, Joule 2, 2618–2632
December 19, 2018
https://doi.org/10.1016/j.joule.2018.09.009

Joule

CellPress

Article

Climatic Impacts of Wind Power

Lee M. Miller[1,3,*] and David W. Keith[1,2,*]

SUMMARY

We find that generating today's US electricity demand (0.5 TW_e) with wind power would warm Continental US surface temperatures by 0.24°C. Warming arises, in part, from turbines redistributing heat by mixing the boundary layer. Modeled diurnal and seasonal temperature differences are roughly consistent with recent observations of warming at wind farms, reflecting a coherent mechanistic understanding for how wind turbines alter climate. The warming effect is: small compared with projections of 21st century warming, approximately equivalent to the reduced warming achieved by decarbonizing global electricity generation, and large compared with the reduced warming achieved by decarbonizing US electricity with wind. For the same generation rate, the climatic impacts from solar photovoltaic systems are about ten times smaller than wind systems. Wind's overall environmental impacts are surely less than fossil energy. Yet, as the energy system is decarbonized, decisions between wind and solar should be informed by estimates of their climate impacts.

INTRODUCTION

To extract energy, all renewables must alter natural energy fluxes, so climate impacts are unavoidable, but the magnitude and character of climate impact varies widely. Wind turbines generate electricity by extracting kinetic energy, which slows winds and modifies the exchange of heat, moisture, and momentum between the surface and the atmosphere. Observations show that wind turbines alter local climate,[1–10] and models show local- to global-scale climate changes from the large-scale extraction of wind power.[11–15] Previous studies have assessed climate impacts of hydropower,[16] biofuels,[17] and solar photovoltaic systems (PVs).[18] Rapid expansion of renewable energy generation is a cornerstone of efforts to limit climate change by decarbonizing the world's energy system. In addition to climate benefits, wind and solar power also reduce emissions of criteria pollutants (NO_x, SO_x, and $PM_{2.5}$) and toxic pollutants such as mercury that cause significant public health impacts.[19,20] The climate impacts of wind and solar are small compared with the impacts of the fossil fuels they displace, but they are not necessarily negligible. Improved understanding of the environmental trade-offs between renewables would inform choices between low-carbon energy sources. With growth of wind and solar PVs far outstripping other renewables,[21] we combine direct observations of onshore wind power's impacts with a continental-scale model, and compare it to prior estimates of PVs' impacts to assess the relative climate impacts of wind and solar energy per unit energy generation.

Climatic impacts due to wind power extraction were first studied using general circulation models (GCMs). These studies found statistically significant climatic impacts within the wind farm, as well as long-distance teleconnections, with impacts outside the wind farm sometimes as large in magnitude as impacts inside the wind farm.[11–13,22] Note that such impacts are unlike greenhouse gas (GHG)-driven warming, as in some cases wind power's climatic impacts might counteract such GHG

Context & Scale

Wind power can impact the climate by altering the atmospheric boundary layer, with at least 40 papers and 10 observational studies now linking wind power to climatic impacts. We make the first comparison between the climatic impacts of large-scale wind power and site-scale observations, finding agreement that warming from wind turbines is largest at night. Wind power's climatic impacts will continue to expand as more are installed.

Do these impacts matter? How do these impacts compare to the climate benefits of reducing emissions? We offer policy-relevant comparisons: wind's climatic impacts are about 10 times larger than solar photovoltaic systems per unit energy generated. We explore the temporal trade-off between wind's climatic impacts and the climate benefits it brings by reducing emissions as it displaces fossil fuels. Quantitative comparisons between low-carbon energy sources should inform energy choices in the transition to a carbon-free energy system.

warming—at least four studies have found that mid-latitude wind power extraction can cool the Arctic.[11,12,23,24] However, these studies often used idealized or unrealistic distributions of turbines installed at unrealistic scales. Model simulations of geometrically simple, isolated wind farms at smaller scales of 3,000–300,000 km^2 (10- to 1,000 times larger than today's wind farms) in windy locations found substantial reductions in wind speed and changes in atmospheric boundary layer (ABL) thickness, as well as differences in temperature,[11,13,14,24] precipitation,[14,25] and vertical atmospheric exchange.[15,26]

We want to assess wind power's climate impacts per unit of energy generation, yet wind's climatic impacts depend on local meteorology and on non-local climate teleconnections. These twin dependencies mean that wind power's impacts are strongly dependent on the amount and location of wind power extraction, frustrating the development of a simple impact metric.

As a step toward an improved policy-relevant understanding, we explore the climatic impacts of generating 0.46 TW_e of wind-derived electricity over the Continental US. This scale fills a gap between the smaller isolated wind farms and global-scale GCM. We model a uniform turbine density within the windiest one-third of the Continental US, and vary the density parametrically.

Our 0.46 TW_e *benchmark scenario* is ~18 times the 2016 US wind power generation rate.[21] We intend it as a plausible scale of wind power generation if wind power plays a major role in decarbonizing the energy system in the latter half of this century. For perspective, the benchmark's electricity generation rate is only 14% of current US primary energy consumption,[25] about the same as US electricity consumption,[27] and about 2.4 times larger than the projected 2050 US wind power generation rate of the *Central Study* in the Department of Energy's (DOE) recent *Wind Vision*.[28] Finally, it is less than one-sixth the technical wind power potential over about the same windy areas of the US as estimated by the DOE.[28,29]

Modeling Framework

We use the WRF v3.3.1 high-resolution regional model[30] with a domain that encompasses the Continental US, forced by boundary conditions from the North American Regional Reanalysis.[31] The *wind farm region* is more than 500 km from the model boundaries, and encompasses only 13% of the domain (shown in Figure 1A). The model configuration used dynamic soil moisture and 31 vertical levels with 3 levels intersecting the turbine's rotor and 8 levels representing the lowermost kilometer. The model is run for a full year after a 1-month spin-up using horizontal resolutions of 10 and 30 km. The wind turbine parametrization was originally released with WRF v3.3,[32] and represents wind turbines as both a momentum sink and turbulent kinetic energy (TKE) source. We updated the wind turbine parameterization to make use of the thrust, power, and TKE coefficients from a Vestas V112 3 MW. This treatment of wind power is very similar to previous modeling studies.[14,15,24]

The advantage of the regional model is that we can use a horizontal and vertical resolution substantially higher than previous global modeling studies,[11–13,22,23,26,33,34] allowing better representation of the interactions of the wind turbines with the ABL. The disadvantage of using prescribed boundary conditions is that our simulations will underestimate the global-scale climatic response to wind power extraction compared with a global model with equivalent resolution, which would allow the global atmosphere to react to the increased surface drag over the US and would reveal climate teleconnections.

[1]School of Engineering and Applied Sciences, Harvard University, Cambridge, MA 02139, USA

[2]Harvard Kennedy School, Cambridge, MA 02138, USA

[3]Lead Contact

*Correspondence: lmiller@seas.harvard.edu (L.M.M.), david_keith@harvard.edu (D.W.K.)

https://doi.org/10.1016/j.joule.2018.09.009

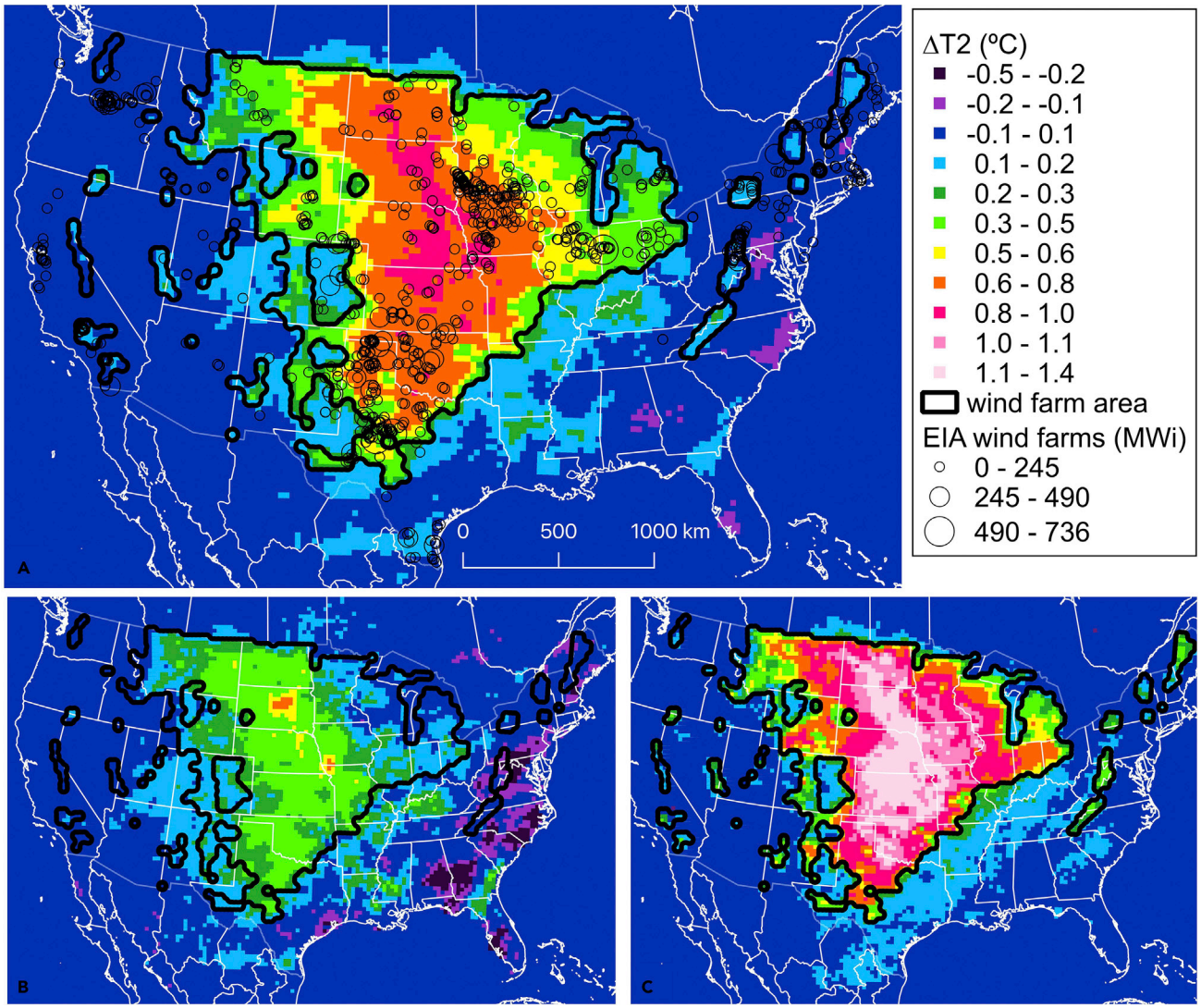

Figure 1. Temperature Response to Benchmark Wind Power Deployment (0.5 MW km^{-2})

(A–C) Maps are 3-year mean of perturbed minus 3-year mean of control for 2-m air temperatures, showing (A) entire period, (B) daytime, and (C) nighttime. The wind farm region is outlined in black, and, for reference, presently operational wind farms are shown as open circles in (A).

We tested horizontal resolution dependence by comparing the 10- and 30-km simulations with a turbine density of 3.0 MW km^{-2} with the respective 2012 controls. Differences in the annual average 2-m air temperature were small, as shown in Figure S1. The following results use a 30-km resolution (about one-ninth of the computational expense) and 2012, 2013, and 2014 simulation periods to reduce the influence of interannual variability. We use four turbine densities (0.5, 1.0, 1.5, and 3.0 MW km^{-2}) within the wind farm region to explore how increased wind power extraction rates alter the climatic impacts.

RESULTS AND DISCUSSION

Figure 1 shows the climate impacts of the benchmark scenario (0.5 MW km^{-2}). The wind farm region experiences warmer average temperatures (Figure 1A), with about twice the warming effect at night compared with during the day (Figures 1B and 1C). Warming was generally stronger nearer to the center of the wind farm region, but

perhaps because teleconnections are suppressed by the forced boundary conditions. The climate response is concentrated in the wind farm region, but there are regions well outside the wind farm region also experiencing a climate response. The clearest example here is along the East Coast during the daytime, where average daytime temperatures are 0.1°C–0.5°C cooler (Figure 1B).

To separate the local direct boundary layer impacts from the mesoscale climate changes, we ran a diagnostic simulation with a 250 × 250-km "hole" near the center of the wind farm region, finding that the "hole" experienced about half the warming of the original "no hole" benchmark scenario during 2014 (Table S1 and Figure S2). This suggests that about half the warming effect is attributed to localized changes in atmospheric mixing, with the other half attributed to mesoscale changes, but this requires further study.

Changes in precipitation are small and show no clear spatial correlation (Figure S3). The warming is greatest in an N-S corridor near the center of the wind turbine array, perhaps because of an interaction between wind turbines and the nocturnal low-level jet (LLJ). The LLJ is a fast nocturnal low-altitude wind (>12 m s^{-1} at 0.5 km) common in the US Midwest, which occurs when the atmosphere decouples from surface friction, resulting in a steep vertical temperature gradient[35]—meteorological conditions that might be sensitive to perturbations by wind turbines. We quantified the presence of the LLJ in our control simulation but did not find a strong spatial correlation between the probability of LLJ occurrence and the nighttime warming (Figure S4). To explore mechanisms, we examine the vertical temperature gradient, atmospheric dissipation, and wind speed (Figure S5), and then explore the relationship between warming and these variables using scatterplots (Figure S6). We find some consistency between the dissipation rate of the control and the warming effect of wind turbines, but the correlation is weak.

Figure 2 explores the relationship between changes in vertical temperature gradient, atmospheric dissipation, and the simulated warming. Wind turbines reduce vertical gradients by mixing. During the day, vertical temperature gradients near the surface are small due to solar-driven convection and are only slightly reduced by the turbines. Gradients are larger at night, particularly during summer, and the gradient reduction caused by turbine-induced mixing is larger. The largest warming occurs when the reduction in gradient is strongest and the proportional increase in TKE is largest.

Warming and power generation saturate with increasing turbine density (Figure 3). The temperature saturation is sharper, so the ratio of temperature change per unit energy generation decreases with increasing turbine density. This suggests that wind's climate impacts per unit energy generation may be somewhat larger for lower values of total wind power production.

Power generation appears to approach the wind power generation limit at turbine densities somewhat above the maximum (3.0 MW km^{-2}) we explored. A capacity density of 1.5 MW_i km^{-2} roughly matches that of US wind farms installed in 2016,[36] and that simulation's power density of 0.46 W_e m^{-2} is very close to the 0.50 W_e m^{-2} observed for US wind farms during 2016.[36] The highest turbine density yields an areal (surface) power density of 0.70 W_e m^{-2}, consistent with some previous studies,[15,22,24,26,33] but half the 1.4 W_e m^{-2} assumed possible by 2050 from the same 3.0 MW km^{-2} turbine density into windy regions by the DOE.[28] While we did not compute a maximum wind power generation rate here, extrapolation of

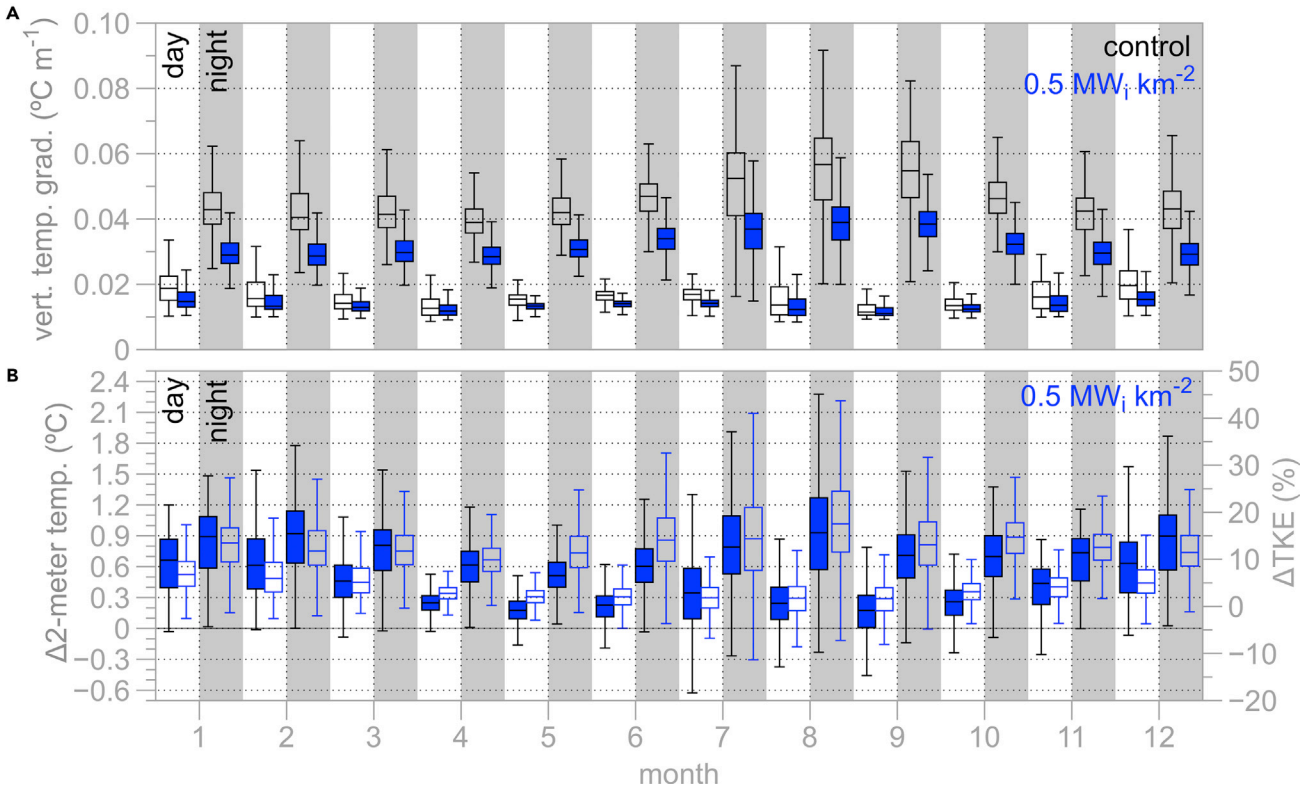

Figure 2. Monthly Day-Night Climate Response to the Benchmark Scenario

(A and B) Average monthly day and night values over the wind farm region for (A) vertical temperature gradient between the lowest two model levels (0–56 and 56–129 m) for the control and benchmark scenario (0.5 $MW_i\ km^{-2}$), and (B) differences between the benchmark scenario and control in 2-m air temperature (solid blue boxes) and turbulent kinetic energy (TKE) in the lowest model level (transparent boxes). In both, the vertical line extent shows the standard 1.5•interquartile range, and the box represents the 25th, 50th, and 75th percentiles.

Figure 3 suggests that it is about 2 TW_e, significantly less than the 3.7 TW_e of technical potential estimated by the DOE[28,29] over less land area. Clearly, interactions of wind turbines with climate must be considered in estimates of technical wind power potential.

Interpretation

The climatic impacts of wind power may be unexpected, as wind turbines only redistribute heat within the atmosphere, and the 1.0 W m^{-2} of heating resulting from kinetic energy dissipation in the lower atmosphere is only about 0.6% of the diurnally averaged radiative flux. But wind's climatic impacts are not caused by additional heating from the increased dissipation of kinetic energy. Impacts arise because turbine-atmosphere interactions alter surface-atmosphere fluxes, inducing climatic impacts that may be much larger than the direct impact of the dissipation alone.

As wind turbines extract kinetic energy from the atmospheric flow and slow wind speeds, the vertical gradient in wind speed steepens, and downward entrainment increases.[15] These interactions increase the mixing between air from above and air near the surface. The strength of these interactions depends on the meteorology and, in particular, the diurnal cycle of the ABL.

During the daytime, solar-driven convection mixes the atmosphere to heights of 1–3 km.[35]

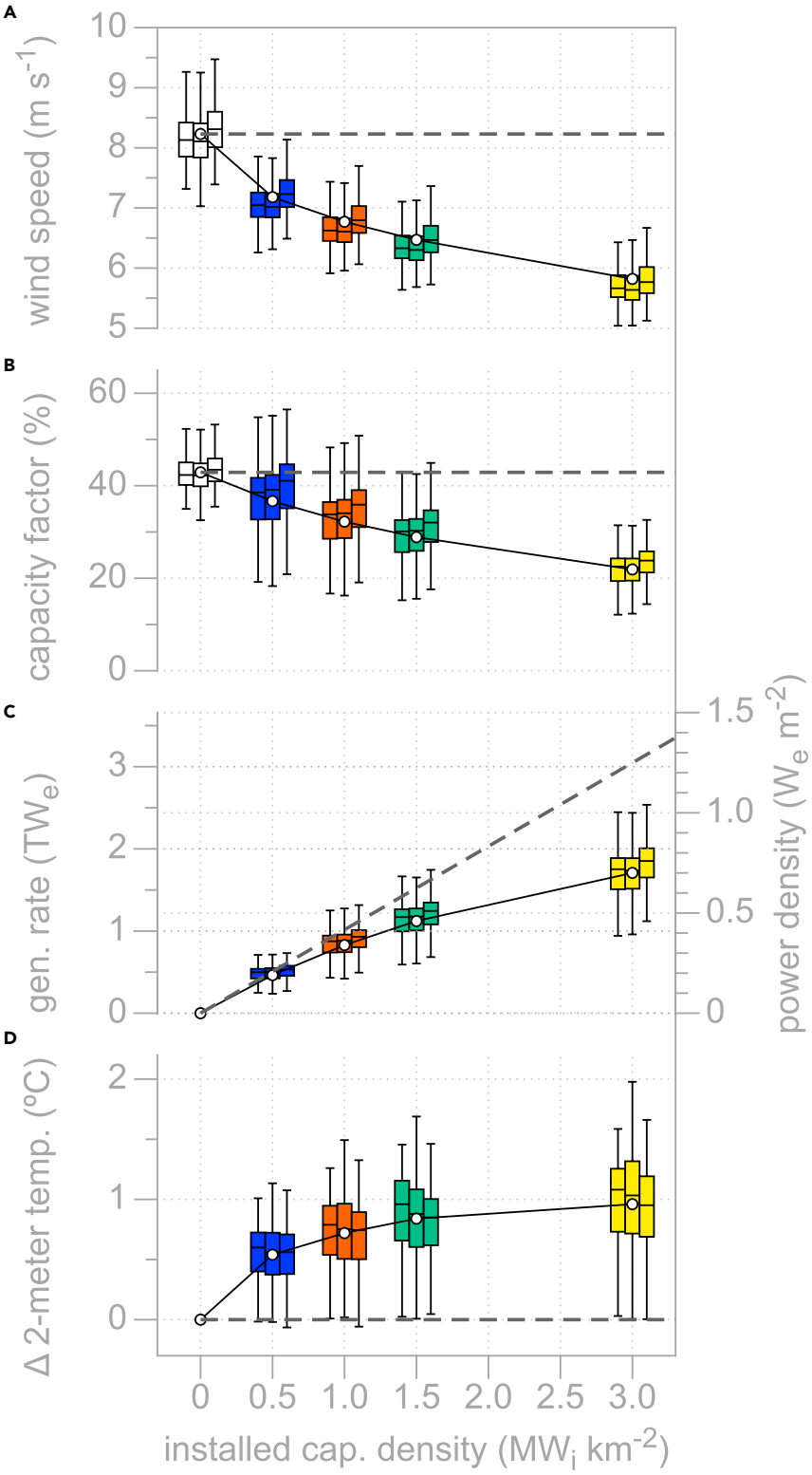

Figure 3. Variation in Mean Response to Changes in Installed Capacity Density

(A–D) The shared x axis is the installed electrical generation capacity per unit area. All values are averages over the wind farm region. (A) Eighty-four-meter hub-height wind speed, (B) capacity

Figure 3. *Continued*
factor, i.e., the ratio of realized electrical output to generation capacity, (C) power output as a sum and per unit area, and (D) difference in 2-m air temperature. For each value, three distinct years of data (2012–2014 from left to right) are shown as three boxplots (1.5•interquartile range, with 25th, 50th, and 75th percentiles). Colors help group identical installed capacity densities. The 3-year mean is shown using white points and connecting solid lines. Dashed lines illustrate the expected results if climate did not respond to the deployment of wind turbines.

Wind turbines operating during the daytime are enveloped within this already well-mixed air, so climatic impacts such as daytime temperature differences are generally quite small. At night, radiative cooling results in more stable surface conditions, with about 100–300 m of stable air separating the influence of surface friction from the winds aloft.[35] Wind turbines operating at night, with physical extents of 100–150 m and an influence height at night reaching 500 m or more,[15] can entrain warmer (potential temperature) air from above down into the previously stable and cooler (potential temperature) air near the surface, warming surface temperatures. In addition to the direct mixing by the turbine wakes, turbines reduce the wind speed gradient below their rotors and thus sharpen the gradient aloft. This sharp gradient may then generate additional turbulence and vertical mixing.

This explanation is broadly consistent with the strong day-night contrast of our benchmark scenario (Figures 1B and 1C). Within the wind farm region during the day, most locations experience warmer air temperatures, although ~15% of locations show a daytime cooling effect in July-September. At night during July-September, less than 5% of locations show a cooling effect, and the warming effect at night over all months is much larger than during the daytime. This daytime and nighttime warming effect is also larger with higher turbine densities (Figure S7). Finally, the temperature perturbation in the benchmark scenario shows a strong correlation to differences in TKE within the lowest model level from 0 to 56 m (Figure 2B), with these increases in TKE downwind of turbines previously observed in Iowa[4] and offshore Germany,[37] and supporting our explanation that the temperature response is driven by increased vertical mixing (Figure 2).

Observational Evidence of Climatic Impacts

While numerous observational studies have linked wind power to reduced wind speeds and increased turbulence in the turbine wakes,[1,4,7,38,39] ten studies have quantified the climatic impacts resulting from these changes (Table 1).

Three ground-based studies have measured differences in surface temperature[1,5,7] and evaporation.[5] Generally, these ground-based observations show minimal climatic impacts during the day, but increased temperatures and evaporation rates at night.

Seven satellite-based studies have quantified surface (skin) temperature differences. By either comparing time periods before and after turbine deployment, or by comparing areas upwind, inside, and downwind of turbines, the spatial extent and intensity of warming for 28 operational wind farms in California,[40] Illinois,[6] Iowa,[2] and Texas[8–10] has been observed. There is substantial consistency between these satellite observations despite the diversity of local meteorology and wind farm deployment scales. Daytime temperature differences were small and slightly warmer and cooler, while nighttime temperature differences were larger and almost always warmer (Table 1). Interpretation of the satellite data is frustrated by fixed overpass times and clouds that sometimes obscure the surface.

Table 1. Overview of Observational Studies Linking Air Temperature Differences to Wind Farms

Reference	SAT or GND	Period	State	Notes: Climatic Impacts within or Very near to the Operational Wind Farm
Baidya Roy and Traiteur,[1] 2010	GND	53 days	CA	summer; ~1°C increase in 5-m air temperature downwind at night through the early morning; slight cooling effect during the day
Walsh-Thomas et al.[40] 2012	SAT	–	CA	~2°C warmer skin temperatures extending to about 2 km downwind, with visible temperature differences to 12 km downwind
Zhou et al.[9] 2012	SAT	9 years	TX	JJA night = +0.72°C, DJF night = +0.46°C; JJA day = −0.04°C; DJF day = +0.23°C; warming is spatially consistent with the arrangement of wind turbines
Zhou et al.[10] 2013	SAT	6 years	TX	QA1 values: DJF night = +0.22°C, MAM night = +0.29°C, JJA night = +0.35°C, SON night = 0.40°C, DJF day = +0.11°C, MAM day = −0.11°C, JJA day = +0.17°C, SON day = −0.04°C
Zhou et al.[10] 2013	SAT	2 years	TX	QA1 values: DJF night = −0.01°C, MAM night = +0.42°C, JJA night = +0.67°C, SON night = 0.47°C, DJF day = +0.14°C, MAM day = −0.42°C, JJA day = +1.52°C, SON day = +0.12°C
Xia et al.[8] 2016	SAT	7 years	TX	DJF night = +0.26°C, MAM night = +0.40°C, JJA night = +0.42°C, SON night = +0.27°C, Annual night = +0.31°C, DJF day = +0.18°C, MAM day = −0.25°C, JJA day = −0.26°C, SON day = −0.02°C, Annual day = −0.09°C
Harris et al.[2] 2014	SAT	11 years	IA	MAM night = +0.07°C, JJA night = +0.17°C, SON night = +0.15°C
Rajewski et al.[4] 2013	GND	122 days	IA	along the edge of a large wind farm directly downwind of ~13 turbines; generally cooler temperatures (0.07°C) with daytime periods that were 0.75°C cooler and nighttime periods that were 1.0–1.5°C warmer
Rajewski et al.[5] 2014	GND	122 days	IA	along the edge of a large wind farm downwind of ~13 turbines co-located with corn and soybeans; night-sensible heat flux and CO_2 respiration increase 1.5–2 times and wind speeds decrease by 25%–50%; daytime H_2O and CO_2 fluxes increase 5-fold 3–5 diameters downwind
Slawsky et al.[6] 2015	SAT	11 years	IL	DJF night = +0.39°C, MAM night = +0.27°C, JJA night = +0.18°C, SON = +0.26°C; Annual = +0.26°C
Smith et al.[7] 2013	GND	47 days	confidential	Spring; nighttime warming of 1.9°C downwind of a ~300 turbine wind farm

SAT, satellite-based observations; GND, ground-based observations. Note that measurements identified as the same state were completed over the same wind farms.

Although our benchmark scenario is very different in scale and turbine placement compared with operational wind power, it is nevertheless instructive to compare our simulation with observations. We compare results at a single Texas location (100.2°W, 32.3°N) where one of the world's largest clusters of operational wind turbines (~200 km^2, consisting of open space and patchy turbine densities of 3.8–4.7 MW km^{-2})[41] has been linked to differences in surface temperature in 3 of the observational studies in Table 1. Weighting the observations by the number of observed-years, the Texas location is 0.01°C warmer during the day and 0.29°C warmer at night (data in Table S2). Our benchmark scenario with a uniform turbine density of 0.5 MW km^{-2} at this location is 0.33°C warmer during the day and 0.66°C warmer at night. To explore the quantitative correlation between the seasonal and diurnal response, we take the 8 seasonal day and night values as independent pairs (Table S2), and find that the observations and the simulations are strongly correlated (Figure 4). This agreement provides strong evidence that the physical mechanisms being modified by the deployment of wind turbines are being captured by our model. This mechanism could be tested more directly if temperature observations upwind and downwind of a large turbine array were available at a high temporal resolution (<3 hr).

Limitations of Model Framework

Climate response is partly related to the choice and placement of wind turbine(s). We modeled a specific 3.0-MW turbine, but future deployment may shift to wind turbines with taller hub heights and larger rotor diameters. We also assumed

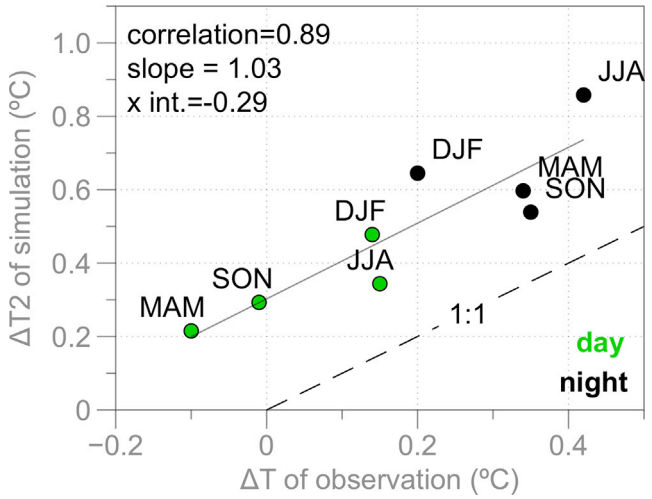

Figure 4. Comparison of Observations and Simulations for the Texas Location (Table 1)
We compare day and night response over four seasons. Observations are surface (skin) temperature differences. Simulation is differences in 2-m air temperatures between the benchmark scenario (0.5 MW km^{-2}) and control. Note that while correlation over eight points is high, the simulated response is larger, likely due to the much larger perturbed area and the difference between skin and 2 m air temperature.

that turbines were evenly spaced over the wind farm region, but real turbine deployment is patchier, potentially also altering turbine-atmosphere-surface interactions.

The model's boundary conditions are prescribed and do not respond to changes caused by wind turbines. Yet prior work has established that non-local climate responses to wind power may be significant,[12] suggesting that simulating our benchmark scenario with a global model (no boundary conditions restoring results to climatology) would allow possible climatic impacts outside the US to be assessed. Removal of the boundary conditions might also increase the warming in the wind farm region. The 3-year simulation period was also completed in 1-year blocks, so we do not simulate the response of longer-term climate dynamics influenced by variables such as soil moisture. Finally, model resolution influenced the estimated climatic impacts. Simulations with a 10-km horizontal resolution and the highest turbine density of 3.0 MW km^{-2} caused 18% less warming than the 30-km simulation (+0.80°C and +0.98°C). Simulations using a global model with an unequally spaced grid with high-resolution over the US could resolve some of these uncertainties.

Comparing Climatic Impacts to Climatic Benefits

Environmental impacts of energy technologies are often compared per unit energy production.[42] Because a central benefit of low-carbon energies like wind and solar is reduced climate change, dimensionless climate-to-climatic comparisons between the climate impacts and climate benefits of reduced emissions are relevant for public policy.

Climate impacts will, of course, depend on a range of climate variables that would need to be examined in a comprehensive impact assessment. In this analysis we nevertheless use 2-m air temperature as a single metric of climate change given (1) that there are important direct impacts of temperature, (2) that temperature

change is strongly correlated with other important climate variables, and (3) that use of temperature as a proxy for other impacts is commonplace in climate impacts assessments. Limitations and caveats of our analysis are addressed in the following sub-section.

When wind (or solar) power replace fossil energy, they cut CO_2 emissions, reducing GHG-driven global climate change, while at the same time causing climatic impacts as described above and elsewhere.[1–15,22–26,34,40,43–45] The climatic impacts differ in (at least) two important dimensions. First, the direct climatic impact of wind power is immediate but would disappear if the turbines were removed, while the climatic benefits of reducing emissions grows with the cumulative reduction in emissions and persists for millennia. Second, the direct climatic impacts of wind power are predominantly local to the wind farm region, while the benefits of reduced emissions are global. We revisit and elaborate these differences in a systematic list of caveats at the end of this subsection.

As a step toward a climate-impact to climate-benefit comparison for wind, we compare warming over the US. We begin by assuming that US wind power generation increases linearly from the current level to 0.46 TW_e in 2080 and is constant thereafter. We estimate the associated warming by scaling our benchmark scenario's temperature differences linearly with wind power generation. The amount of avoided emissions—and thus the climate benefit—depends on the emissions intensity of the electricity that wind displaces. We bracket uncertainties in the time evolution of the carbon-intensity of US electric power generation in the absence of wind power by using two pathways. One pathway assumes a static emissions intensity at the 2016 value (0.44 $kgCO_2\ kWh^{-1}$), while the second pathway's emissions intensity decreases linearly to zero at 2100, which is roughly consistent with the GCAM model[46] that meets the IPCC RCP4.5 scenario. The two emissions pathways are then reduced by the (zero emission) wind power generation rate at that time (Figure 5C). The first pathway likely exaggerates wind power's emission reductions, while the second reflects reduced climate-benefit for wind in a transition to a zero-carbon grid that might be powered by solar or nuclear.

It is implausible that the US would make deep emissions cuts while the rest of the world continues with business-as-usual, so we include a third pathway, which functions just like the first pathway, except that the global (rather than just US) electricity emissions intensity declines to zero (Figure S8)

We estimate wind's reduction in global warming by applying the two US and one global emission pathways to an emissions-to-climate impulse response function.[47] We convert these global results to a US warming estimate using the 1.34:1 ratio of US-to-global warming from IPCC RCP4.5 and RCP8.5 ensemble means (Figure S9,[48]).

The benchmark scenario's warming of 0.24°C over the Continental US and 0.54°C over the wind farm region are small-to-large depending on the baseline. Climatic impacts are small if compared with US temperature projections— historical and ongoing global emissions are projected to cause the Continental US to be 0.24°C warmer than today by the year 2030 (Figure S8). Assuming emissions cuts are implemented globally, then the climatic impacts of wind power affecting the US in 2100 are approximately equivalent to the avoided warming from reduced global emissions (green region of Figure 5D). Climatic impacts are large if the US is the only country reducing emissions over this century (blue and gray shaded regions of

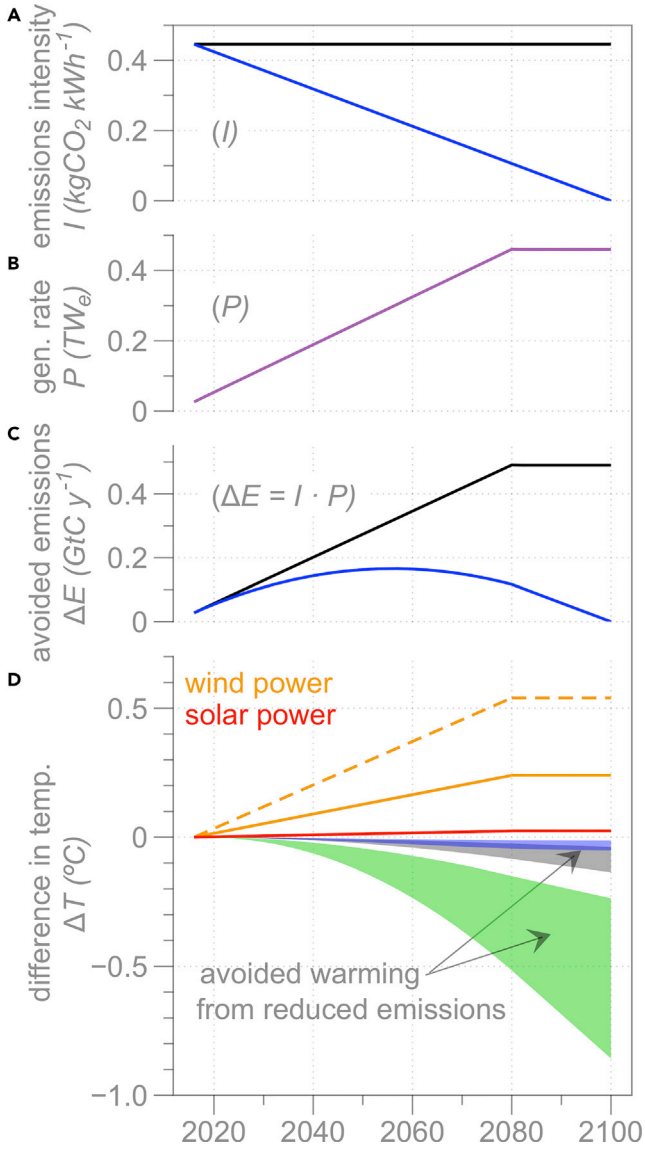

Figure 5. Climate Warming Impacts Compared to Climate Benefits of Reduced Emissions

(A) Two US scenarios, static (black) and declining (blue) emissions intensity, *I*, from US electric power.

(B) A scenario in which power output, *P*, from wind or solar power increases to our benchmark scenario's 0.46 TWe by 2080.

(C and D) Avoided emissions computed as $\Delta E = I \times P$ (C) and the resulting 2-m temperature differences within the wind farm region (dotted lines) and the Continental US (solid lines) (D). Values for wind power linearly scaled from our benchmark scenario, while values for solar power are derived from Nemet.[18] For comparison, the avoided warming of the Continental US from reduced emissions is shown for the static US scenario (gray) and the declining US scenario (blue). The green area shows the avoided warming of the Continental US if global electricity emissions were zero by 2080. The range of avoided warming for each pathway is estimated from the min and max values within the emissions-to-climate impulse response function.

Figure 5D). Timescale matters because climatic impacts are immediate, while climate benefits grow slowly with accumulated emission reductions. The longer the time horizon, the less important wind power's impacts are compared with its benefits (Box 1).

Box 1. Limitations of Using these Results to Compare the Climatic Impacts of Wind Power to Climate Change from Long-Lived Greenhouse Gases

The comparison above suggests that if US electricity demand was met with US-based wind power, the wind farm array would need to operate for more than a century before the warming effect over the Continental US caused by turbine-atmosphere interactions would be smaller than the reduced warming effect from lowering emissions. This conclusion is subject to a number of caveats including:

- Fundamentally different mechanisms cause warmer temperatures from climate change compared with wind power. Increased GHG concentrations reduce radiative heat losses to space, trapping more heat in the atmosphere and causing warmer surface temperatures. Wind power does not add more heat to the atmosphere—wind turbines redistribute heat by mixing and alter large-scale flows both which can change climate.
- Our comparison was based solely on surface air temperature differences. Wind turbines and GHGs both alter a host of interrelated climate variables. The use of surface temperature as the sole proxy for climate impacts may bias the resulting ratio of impacts-to-benefits in either direction.
- Climate impacts of the benchmark scenario will likely be larger and more widespread if we did not use forced boundary conditions, which prevents any feedbacks from the large-scale circulation.
- Results depend on the wind electricity generation rate, consistent with previous work.[11] Our results (Figure 3) suggest the temperature response is *roughly* linear to the generation rate and power density. To the extent that we see deviations from linearity (Figure S7), climate impacts per unit generation are larger for lower turbine densities.
- Results depend on the spatial distribution and density of wind turbines. We assumed that the windiest areas would be exploited and that developers would use low turbine densities to maximize per-turbine generation. Based on simulated results with higher turbine densities (Figure 3), doubling the turbine density over an area half as large as the benchmark scenario might generate almost the same power as the benchmark scenario, while increasing warming over this smaller region by only about a third.
- Our comparison metric ignores many possible benefits and drawbacks of the climate impacts caused by wind power deployment, including:
  - Arctic cooling shown in most large-scale wind power modeling studies.[11,23,24,45]
  - Warmer minimum daily temperatures reduce the incidence and severity of frost, and lengthen the growing season. Compared to the control, the growing season of the wind farm region was 8 days longer in our benchmark scenario, and 13 days longer with 3.0 $MW_i\ km^{-2}$.
  - Some locations experience cooler average temperatures during the summer (Figure 2B), consistent with observations,[1,4] and could reduce heat stress.
  - Warmer minimum daily temperatures have been observed to reduce crop yield.[49]
  - Warmer minimum temperatures could influence insect life history in unknown ways.[50]
- The comparison depends on area-weighting. We used equal weighting but one could consider weighting by, for example, population or agricultural production.
- The comparison depends very strongly on the time horizon. We examined the century timescale consistent with Global Warming Potentials, but there is no single right answer for time discounting.[51,52]
- Finally, results depend on the comparison of US and global-scale impacts and benefits: our model framework prevents global-scale analyses, but, assuming a substantial fraction of the warming effect occurred where US wind turbines were operating, global area-weighted benefits would offset the climatic impacts sooner than if impacts and benefits were quantified over just the US (as done here).

Implications for Energy System Decarbonization

Wind beats fossil fuels under any reasonable measure of long-term environmental impacts per unit of energy generated. Assessing the environmental impacts of wind power is relevant because, like all energy sources, wind power causes climatic impacts. As society decarbonizes energy systems to limit climate change, policy makers will confront trade-offs between various low-carbon energy technologies such as wind, solar, biofuels, nuclear, and fossil fuels with carbon capture. Each technology benefits the global climate by reducing carbon emissions, but each also causes local environmental impacts.

Our analysis allows a simple comparison of wind power's climate benefits and impacts at the continental scale. As wind and solar are rapidly growing sources of low-carbon electricity, we compare the climate benefit-to-impact ratio of wind and solar power.

The climate impacts of solar PVs arise from changes in solar absorption (albedo). A prior study estimated that radiative forcing per unit generation increased at 0.9 mWm^{-2}/TW_e, in a scenario in which module efficiency reaches 28% in 2100 with installations over 20% rooftops, 40% grasslands, and 40% deserts.[18] Assuming that the climatic impact is localized to the deployment area and using a climate

sensitivity of 0.8K/Wm^{-2},[53] generating 0.46 TW$_e$ of solar PVs would warm the Continental US by 0.024°C. This warming effect is 10-times smaller than wind's (0.24°C, Figure 5D) for the same energy generation rate. This contrast is linked to differences in power density and thus to the areal footprint per unit energy—US solar farms presently generate about 5.4 W$_e$ m^{-2}, while US wind farms generate about 0.5 W$_e$ m^{-2}.[36] We speculate that solar PVs' climatic impacts might be reduced by choosing low albedo sites to reduce impacts or by altering the spectral reflectivity of panels. Reducing wind's climatic impacts may be more difficult, but might be altered by increasing the height of the turbine rotor above the surface distance to reduce interactions between the turbulent wake and the ground, or switching the turbines on or off depending on meteorological conditions.

In agreement with observations and prior model-based analyses, US wind power will likely cause non-negligible climate impacts. While these impacts differ from the climate impacts of GHGs in many important respects, they should not be neglected. Wind's climate impacts are large compared with solar PVs. Similar studies are needed for offshore wind power, for other countries, and for other renewable technologies. There is no simple answer regarding the *best* renewable technology, but choices between renewable energy sources should be informed by systematic analysis of their generation potential and their environmental impacts.

SUPPLEMENTAL INFORMATION

Supplemental Information includes nine figures and two tables and can be found with this article online at https://doi.org/10.1016/j.joule.2018.09.009.

ACKNOWLEDGMENTS

We thank A. Karmalkar for providing ensemble mean surface temperature data for the IPCC RCP4.5 and RCP8.5 projections,[48] S. Leroy and N. Brunsell for technical assistance, and J. Holdren, S. Pacala, and three anonymous reviewers for constructive comments on the manuscript. This work was supported by the Fund for Innovative Climate and Energy Research.

AUTHOR CONTRIBUTIONS

Conceptualization, L.M.M. and D.W.K.; Methodology, L.M.M.; Investigation, L.M.M. and D.W.K.; Writing – Original Draft, L.M.M. and D.W.K.; Writing – Review & Editing, L.M.M. and D.W.K.; Visualization, L.M.M. and D.W.K.; Funding Acquisition, D.W.K.

DECLARATION OF INTERESTS

D.W.K. is an employee, shareholder, and executive board member at Carbon Engineering (Squamish, BC). Carbon Engineering is developing renewable electricity to fuels projects and is developing procurement contracts for wind and solar power.

Received: May 4, 2018
Revised: August 16, 2018
Accepted: September 13, 2018
Published: October 4, 2018

REFERENCES

1. Baidya Roy, S., and Traiteur, J. (2010). Impacts of wind farms on surface air temperatures. Proc. Natl. Acad. Sci. USA *107*, 17899–17904.

2. Harris, R.A., Zhou, L., and Xia, G. (2014). Satellite observations of wind farm impacts on nocturnal land surface temperature in Iowa. Rem. Sens. *6*, 12234–12246.

3. Hasager, C.B., Vincent, P., Badger, J., Badger, M., Di Bella, A., Peña, A., Husson, R., and Volker, P. (2015). Using satellite SAR to characterize the wind flow around

offshore wind farms. Energies *8*, 5413–5439.

4. Rajewski, D.A., Takle, E.S., Lundquist, J.K., Oncley, S., Prueger, J.H., Horst, T.W., Rhodes, M.E., Pfeiffer, R., Hatfield, J.L., Spoth, K.K., et al. (2013). Crop wind energy experiment (CWEX): observations of surface-layer, boundary layer, and mesoscale interactions with a wind farm. Bull. Am. Meteorol. Soc. *94*, 655–672.

5. Rajewski, D.A., Takle, E.S., Lundquist, J.K., Prueger, J.H., Pfeiffer, R.L., Hatfield, J.L., Spoth, K.K., and Doorenbos, R.K. (2014). Changes in fluxes of heat, H_2O, and CO_2 caused by a large wind farm. Agric. For. Meteorol. *194*, 175–187.

6. Slawsky, L.M., Zhou, L., Baidya Roy, S., Xia, G., Vuille, M., and Harris, R.A. (2015). Observed thermal impacts of wind farms over Northern Illinois. Sensors (Basel) *15*, 14981–15005.

7. Smith, C.M., Barthelmie, R.J., and Pryor, S.C. (2013). In situ observations of the influence of a large onshore wind farm on near-surface temperature, turbulence intensity and wind speed profiles. Environ. Res. Lett. *8*, 034006.

8. Xia, G., Zhou, L., Freedman, J., and Baidya Roy, S. (2016). A case study of effects of atmospheric boundary layer turbulence, wind speed, and stability on wind farm induced temperature changes using observations from a field. Clim. Dyn. *46*, 2179–2196.

9. Zhou, L., Tian, Y., Baidya Roy, S., Thorncroft, C., Bosart, L.F., and Hu, Y. (2012). Impacts of wind farms on land surface temperature. Nat. Clim. Chang. *2*, 539–543.

10. Zhou, L., Tian, Y., Baidya Roy, S., Dai, Y., and Chen, H. (2013). Diurnal and seasonal variations of wind farm impacts on land surface temperature over western Texas. Clim. Dyn. *41*, 307–326.

11. Keith, D.W., Decarolis, J.F., Denkenberger, D.C., Lenschow, D.H., Malyshev, S.L., Pacala, S., and Rasch, P.J. (2004). The influence of large-scale wind power on global climate. Proc. Natl. Acad. Sci. USA *101*, 16115–16120.

12. Kirk-Davidoff, D., and Keith, D.W. (2008). On the climate impact of surface roughness anomalies. J. Atmos. Sci. *65*, 2215–2234.

13. Wang, C., and Prinn, R.G. (2010). Potential climatic impacts and reliability of very large-scale wind farms. Atmos. Chem. Phys. *10*, 2053–2061.

14. Vautard, R., Thais, F., Tobin, I., Bréon, F.M., Devezeaux de Lavergne, J.G., Colette, A., Yiou, P., and Ruti, P.M. (2014). Regional climate model simulations indicate limited climatic impacts by operational and planned European wind farms. Nat. Commun. *5*, 3196.

15. Miller, L.M., Brunsell, N.A., Mechem, D.B., Gans, F., Monaghan, A.J., Vautard, R., Keith, D.W., and Kleidon, A. (2015). Two methods for estimating limits to large-scale wind power generation. Proc. Natl. Acad. Sci. USA *112*, 11169–11174.

16. Deemer, B.R., Harrison, J.A., Li, S., Beaulieu, J.J., Delsontro, T., Barros, N., Bezerra-Neto, J.F., Powers, S.M., Dos Santos, M.A., and Arie Vonk, J. (2016). Greenhouse gas emissions from reservoir water surfaces: a new global synthesis. BioScience *66*, 949–964.

17. Searchinger, T., Heimlich, R., Houghton, R.A., Dong, F., Elobeid, A., Fabiosa, J., Tokgoz, S., Hayes, D., and Yu, T.H. (2008). Use of U.S. croplands for biofuels increases greenhouse gases through emissions from land-use change. Science *319*, 1238–1240.

18. Nemet, G.F. (2009). Net radiative forcing from widespread deployment of photovoltaics. Environ. Sci. Technol. *43*, 2173–2178.

19. Siler-Evans, K., Lima, I., Morgan, M.G., and Apt, J. (2013). Regional variations in the health, environmental, and climate benefits of wind and solar generation. Proc. Natl. Acad. Sci. USA *110*, 11768–11773.

20. Millstein, D., Wiser, R., Bolinger, M., and Barbose, G. (2017). The climate and air-quality benefits of wind and solar power in the United States. Nat. Energy *2*, 17134.

21. US Energy Information Administration (2017). Electric Power Monthly (EIA Publication). www.eia.gov/electricity/monthly/pdf/epm.pdf.

22. Miller, L.M., Gans, F., and Kleidon, A. (2011). Estimating maximum global land surface wind power extractability and associated climatic consequences. Earth Syst. Dynam. *2*, 1–12.

23. Marvel, K., Kravitz, B., and Caldeira, K. (2012). Geophysical limits to global wind power. Nat. Clim. Chang. *2*, 1–4.

24. Adams, A.S., and Keith, D.W. (2013). Are global wind power resource estimates overstated? Environ. Res. Lett. *8*, 015021.

25. Fiedler, B.H., and Bukovsky, M.S. (2011). The effect of a giant wind farm on precipitation in a regional climate model. Environ. Res. Lett. *6*, 045101.

26. Miller, L.M., and Kleidon, A. (2016). Wind speed reductions by large-scale wind turbine deployments lower turbine efficiencies and set low generation limits. Proc. Natl. Acad. Sci. USA *113*, 13570–13575.

27. US Energy Information Administration (2017). U.S. Primary Energy Consumption by Source and Sector, 2016 (EIA Publication). www.eia.gov/totalenergy/data/monthly/pdf/flow/css_2016_energy.pdf.

28. US Dept. of Energy (2015). Wind Vision: A New Era for Wind Power in the United States (DOE Publication). www.energy.gov/sites/prod/files/WindVision_Report_final.pdf.

29. Lopez, A., Roberts, B., Heimiller, D., Blair, N., and Porro, G. 2012. U.S. renewable energy technical potentials : a GIS-based analysis. DOE Tech. Rep. TP-6A20–51946. www.nrel.gov/docs/fy12osti/51946.pdf.

30. Skamarock, W.C., Klemp, J.B., Dudhia, J., Gill, D.O., Barker, D.M., Duda, M.G., Huang, X., Wang, W., and Powers J.G. A Description of the Advanced Research WRF Version 3. NCAR technical note NCAR/TN-475+STR. National Center for Atmospheric Research.

31. Mesinger, F., DiMego, G., Kalnay, E., Mitchell, K., Shafran, P.C., Ebisuzaki, W., Jović, D., Woollen, J., Rogers, E., and Berbery, E.H. (2006). North American regional reanalysis. Bull. Am. Meteorol. Soc. *87*, 343–360.

32. Fitch, A.C., Olson, J.B., Lundquist, J.K., Dudhia, J., Gupta, A.K., Michalakes, J., and Barstad, I. (2012). Local and mesoscale impacts of wind farms as parameterized in a mesoscale NWP model. Mon. Weather Rev. *140*, 3017–3038.

33. Jacobson, M.Z., and Archer, C.L. (2012). Saturation wind power potential and its implications for wind energy. Proc. Natl. Acad. Sci. USA *109*, 15679–15684.

34. Barrie, D.B., and Kirk-Davidoff, D.B. (2010). Weather response to management of a large wind turbine array. Atmos. Chem. Phys. *10*, 769–775.

35. Garratt, J.R. (1994). The Atmospheric Boundary Layer (Cambridge University Press).

36. Miller, L.M., and Keith, D.W. (2018). Observation-based solar and wind power capacity factors and power densities. ERL. Published online October 4, 2018. https://doi.org/10.1088/1748-9326/aae102.

37. Platis, A., Siedersleben, S.K., Bange, J., Lampert, A., Bärfuss, K., Hankers, R., Cañadillas, B., Foreman, R., Schulz-Stellenfleth, J., Djath, B., et al. (2018). First in situ evidence of wakes in the far field behind offshore wind farms. Sci. Rep. *8*, 2163.

38. Hirth, B.D., Schroeder, J.L., Gunter, W.S., and Guynes, J.G. (2012). Measuring a utility-scale turbine wake using the TTUKa mobile research radars. J. Atmos. Ocean. Technol. *29*, 765–771.

39. Iungo, G.V., Wu, Y., and Porté-Agel, F. (2013). Field measurements of wind turbine wakes with lidars. J. Atmos. Ocean. Technol. *30*, 274–287.

40. Walsh-Thomas, J.M., Cervone, G., Agouris, P., and Manca, G. (2012). Further evidence of impacts of large-scale wind farms on land surface temperature. Renew. Sustain. Energy Rev. *16*, 6432–6437.

41. Denholm, P., Hand, M., Jackson, M., and Ong, S. 2009. Land-use requirements of modern wind power plants in the United States. DOE Tech. Rep. NREL/TP-6A2–45834. www.nrel.gov/docs/fy09osti/45834.pdf.

42. Deschênes, O., and Greenstone, M. (2011). Climate change, mortality, and adaptation: evidence from annual fluctuations in weather in the US. Am. Econ. J. Appl. Econ. *3*, 152–185.

43. Christiansen, M.B., and Hasager, C.B. (2005). Wake effects of large offshore wind farms identified from satellite SAR. Remote Sens. Environ. *98*, 251–268.

44. Jacobson, M.Z., Archer, C.L., and Kempton, W. (2014). Taming hurricanes with arrays of offshore wind turbines. Nat. Clim. Chang. *4*, 195–200.

45. Possner, A., and Caldeira, K. (2017). Geophysical potential for wind energy over the open oceans. Proc. Natl. Acad. Sci. USA *114*, 11338–11343.

46. Moss, R.H., Edmonds, J.A., Hibbard, K.A., Manning, M.R., Rose, S.K., van Vuuren, D.P., Carter, T.R., Emori, S., Kainuma, M., Kram, T., et al. (2010). The next generation of scenarios for climate change research and assessment. Nature *463*, 747–756.

47. Ricke, K.L., and Caldeira, K. (2014). Maximum warming occurs about one decade after a carbon dioxide emission. Environ. Res. Lett. *9*, 124002.

48. Karmalkar, A.V., and Bradley, R.S. (2017). Consequences of global warming of 1.5°C and 2°C for regional temperature and precipitation changes in the Contiguous United States. PLoS One *12*, e0168697.

49. Hatfield, J.L., Boote, K.J., Kimball, B.A., Ziska, L.H., and Izaurralde, R.C. (2011). Climate impacts on agriculture: implications for crop production. Agron. J. *103*, 351.

50. Chen, S., Fleischer, S.J., Saunders, M.C., and Thomas, M.B. (2015). The influence of diurnal temperature variation on degree-day accumulation and insect life history. PLoS One *10*, e0120772.

51. Kirschbaum, M.U.F. (2014). Climate-change impact potentials as an alternative to global warming potentials. Environ. Res. Lett. *9*, 034014.

52. Ocko, I.B., Hamburg, S.P., Jacob, D.J., Keith, D.W., Keohane, N.O., Oppenheimer, M., Roy-Mayhew, J.D., Schrag, D.P., and Pacala, S.W. (2017). Unmask temporal trade-offs in climate policy debates. Science *356*, 492–493.

53. Rahmstorf, S. (2008). Anthropogenic climate change: revisiting the facts. In Global Warming: Looking Beyond Kyoto, E. Zedillo, ed. (Brookings Institution Press), pp. 34–53.

JOUL, Volume *2*

Supplemental Information

Climatic Impacts of Wind Power

Lee M. Miller and David W. Keith

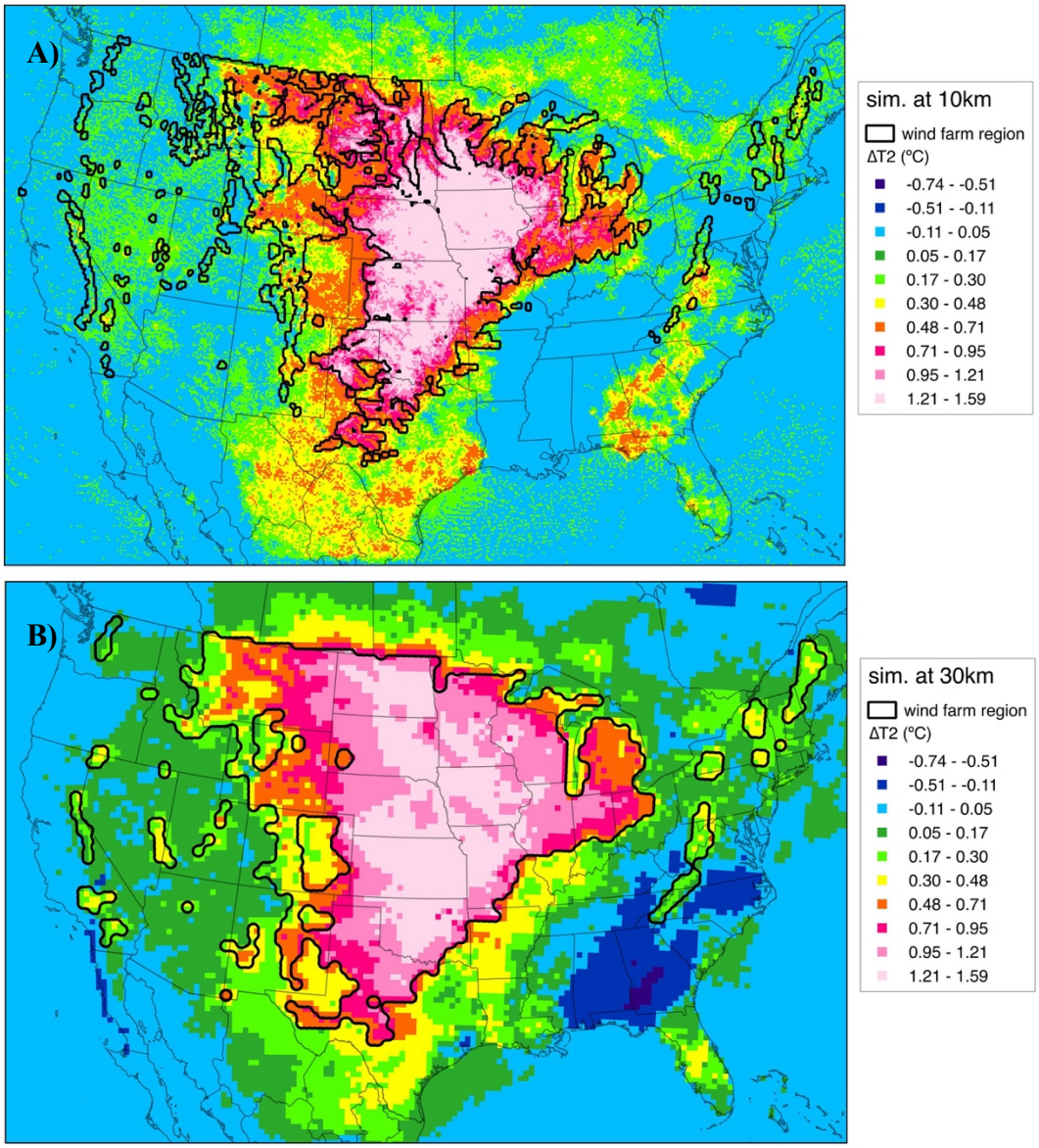

Fig. S1.

Annual mean 2-meter air temperature differences over 2012 resulting from the deployment of a turbine density of 3 MW km^{-2} into the *wind farm regions* (black outlined areas), simulated using **A)** 10 km horizontal resolution, and **B)** 30 km horizontal resolution. The wind farm regions are spatially different. Based on control conditions, the wind farm region in the 10 km simulation encompasses 27% of the Continental US (*i.e.* 2012 mean 80 meter wind speed greater than 7.6 m s^{-1}). The wind farm region of the 30 km simulation encompasses 31% of the Continental US land area, and is identified as the 2012-2014 mean 80-meter wind speed greater than 7.5 m s^{-1}.

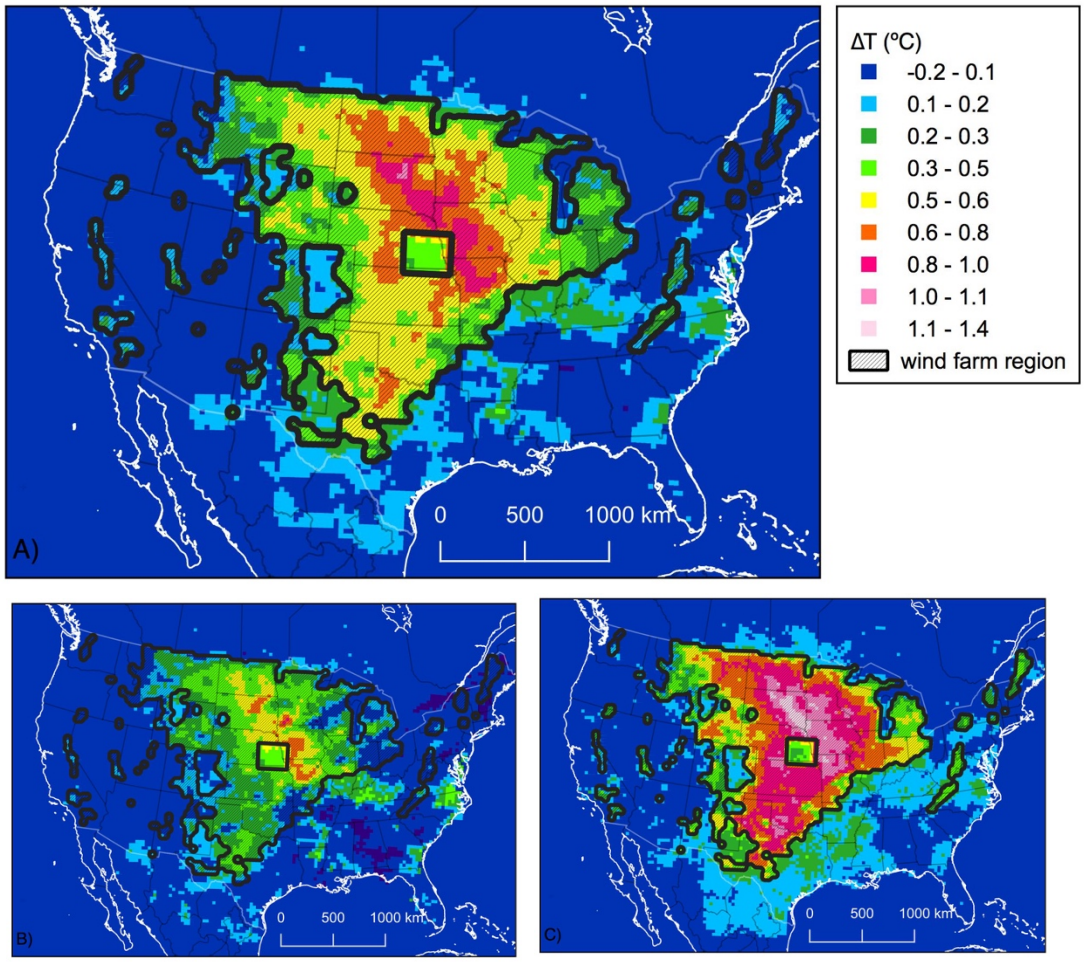

Fig. S2.

2-meter air temperature response to benchmark wind power deployment (0.5 MW_i km^{-2}), but with a 250x250km absence of wind turbines in southeast Nebraska and comparing the year 2014. This is in contrast to Figure 1 of the main text, where the Nebraska hole is not included and a 3-year (2012-2014) is shown. Maps are annual means over 2014 of perturbed minus control for 2-meter air temperatures, showing **(A)** entire period, **(B)** daytime, and **(C)** nighttime. The wind farm region is outlined in black. Mean values within the hole are noted in Table S1.

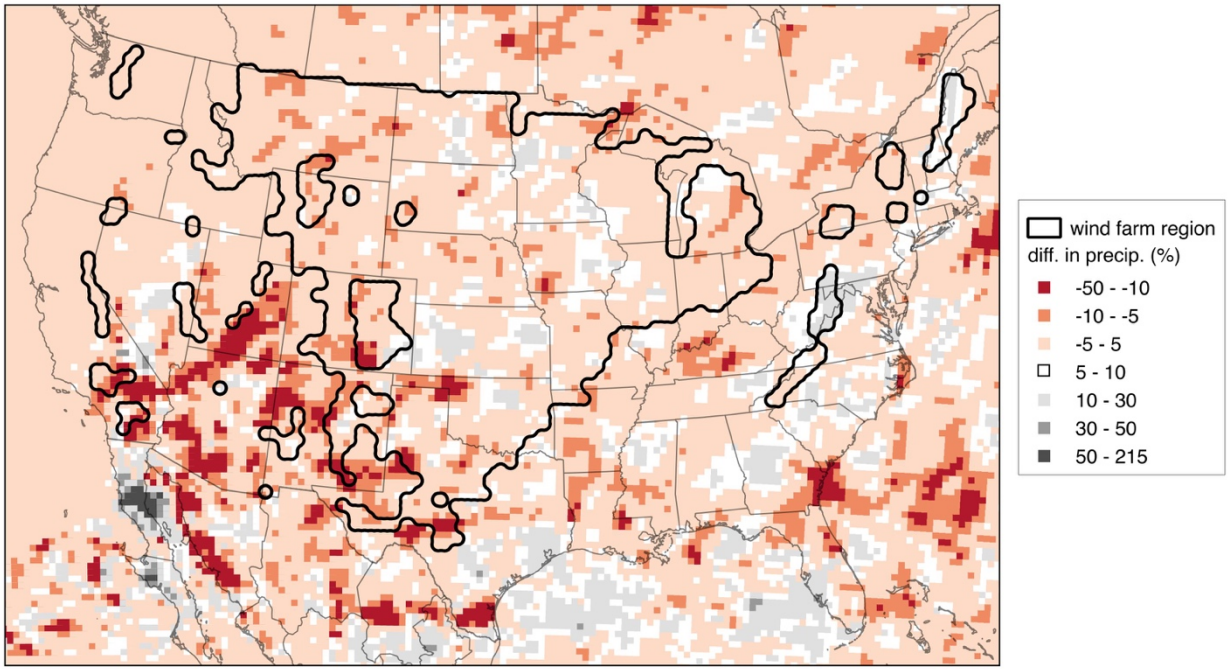

Fig. S3

Mean (2012-2014) precipitation differences between the *benchmark scenario* (0.5 MW km^{-2}) and the control. The black outlined area delineates the wind farm region. Overall, precipitation increased by 2% within the wind farm region.

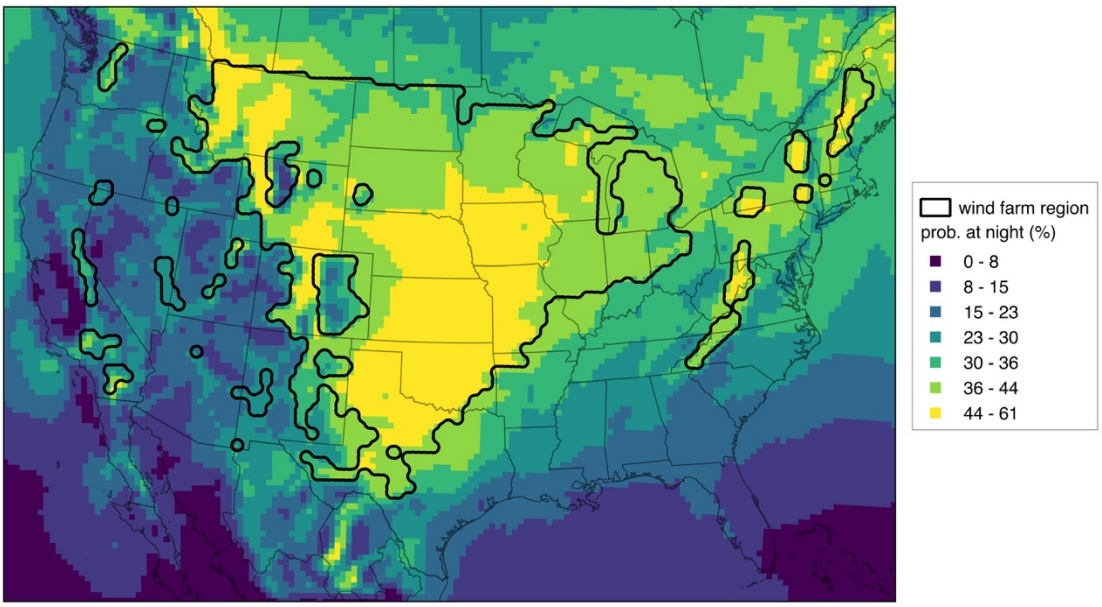

Fig. S4

Probability of the LLJ at night over the 3-year (2012-2014) period based on control conditions, defined as wind speeds greater than 12 m s^{-1} within 500m of the ground surface. The wind farm region is outlined in black.

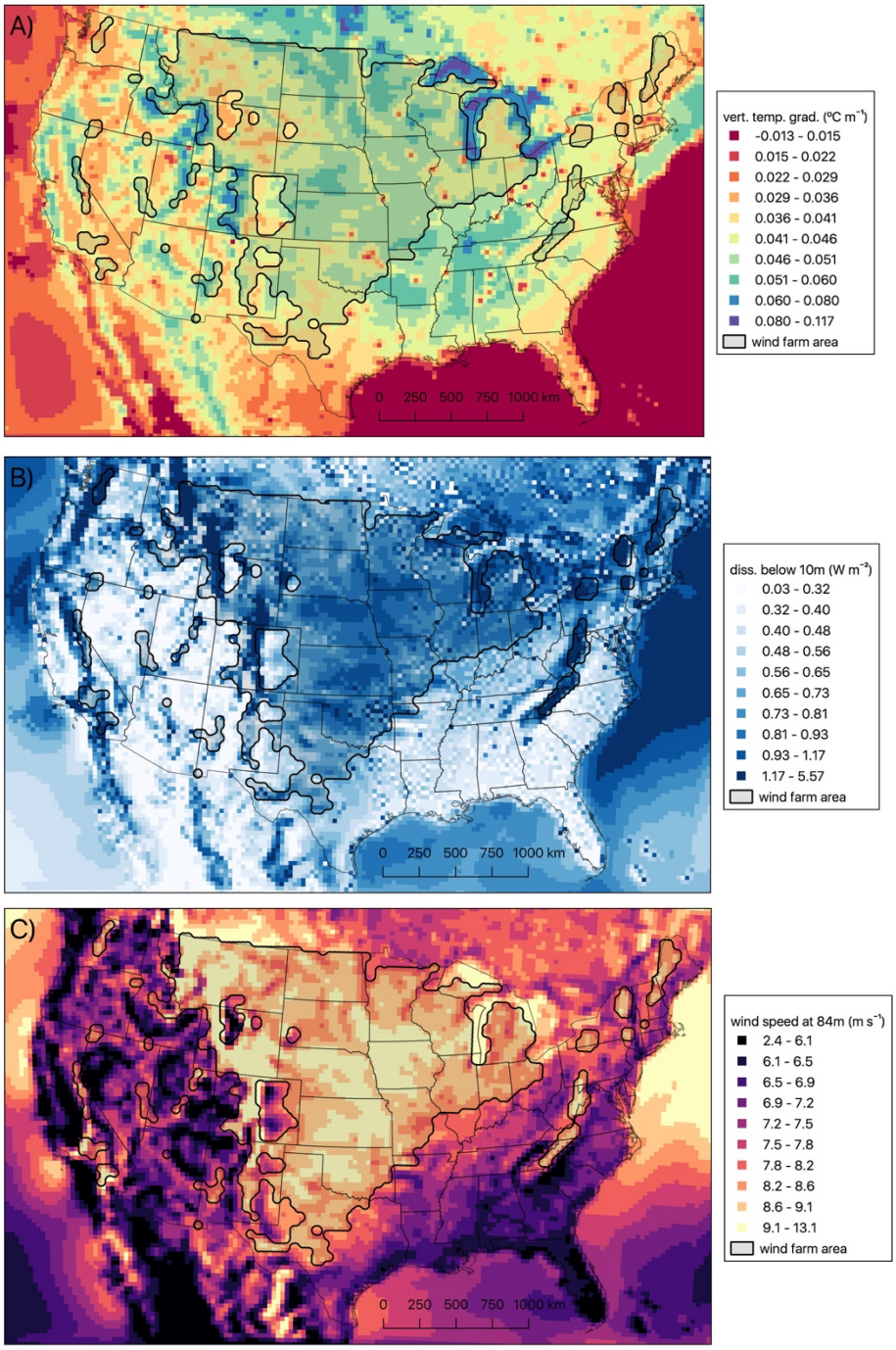

Fig. S5

3-year mean conditions at night of the control simulation to help understand the spatial pattern of nighttime warming (main text Fig. 1C), **A)** vertical gradient in virtual potential temperature between the lowest two model levels (0-56m, 56-129m), **B)** surface dissipation within 10m of the surface, derived as $\boldsymbol{\rho} u_*^2 \cdot (v_{10})$, where $\boldsymbol{\rho}$ is the air density, u_* is the friction velocity, and v_{10} is the 10-meter wind speed, **C)** 84-meter wind speed (hub-height of the wind turbines). Note, the spottiness in B&C corresponds to cities in the US Midwest and Southeast.

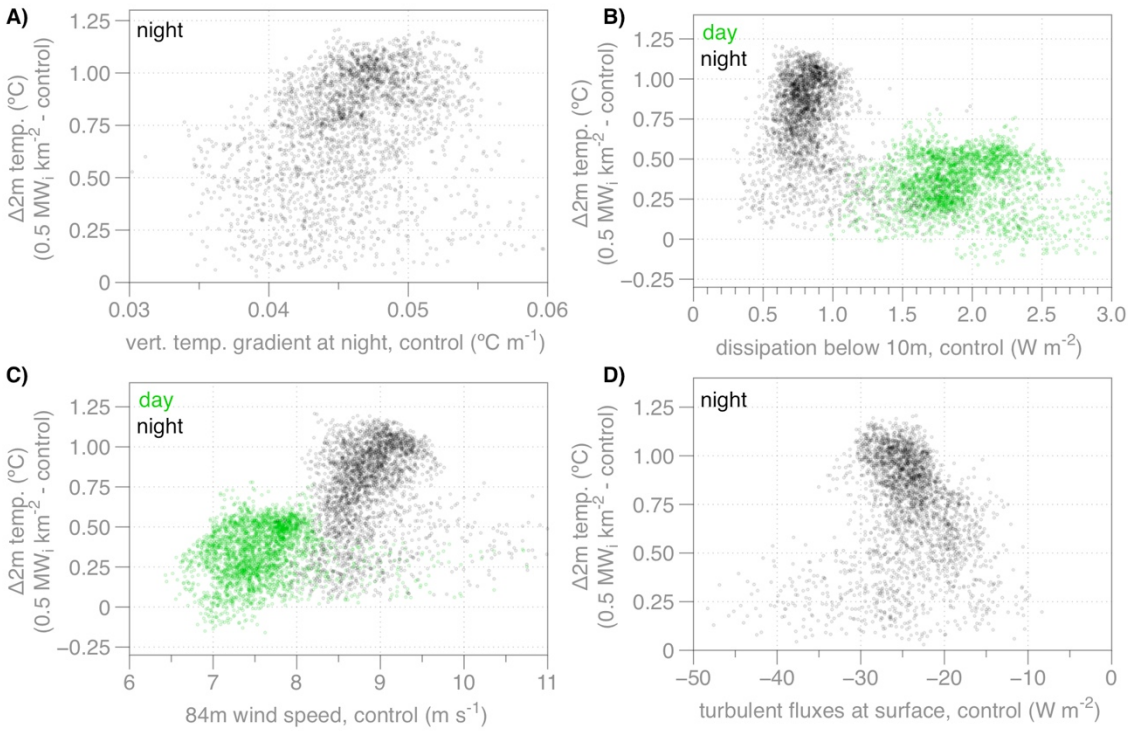

Fig. S6

Comparing 3-year means of control variables to differences in 2-meter air temperature between the benchmark scenario (0.5 MW_i km^{-2}) and the control for each grid point within the wind farm region. **A)** vertical temperature gradient between the lowest 2 model levels (0-56m, 56-129m), **B)** dissipation within 10m of the surface, derived as $\boldsymbol{\rho} u_*^2 \cdot (v_{10})$, where $\boldsymbol{\rho}$ is the air density, u_* is the friction velocity, and v_{10} is the 10-meter wind speed, **C)** 84-meter (hub-height) wind speed, and **D)** turbulent fluxes (sensible heat flux + latent heat flux). 'Night' values in A,B,C correspond to the maps in Fig. S5.

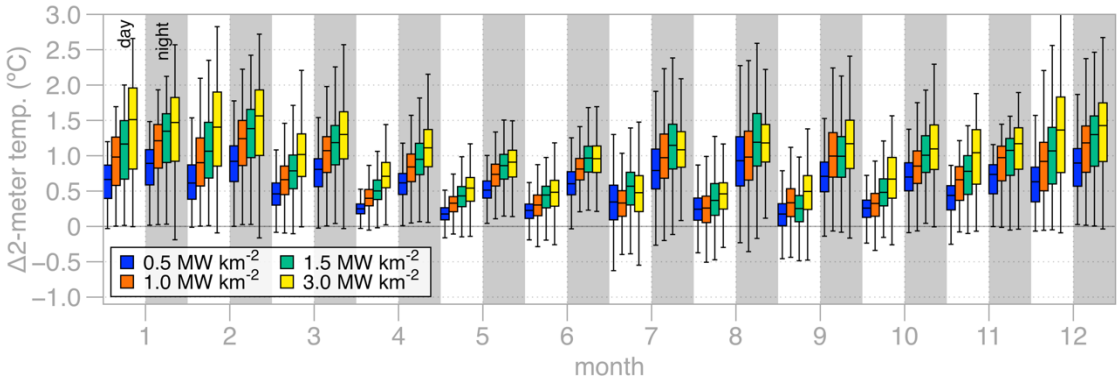

Fig. S7

Day and night 3-year monthly mean 2-meter air temperature differences over the wind farm region between the various turbine densities and the control simulation. The blue box-whisker plot data is the same at in Fig. 1D. The vertical line extent encompasses 1.5-times the interquartile range and the box represents the 25th, 50th, and 75th percentiles.

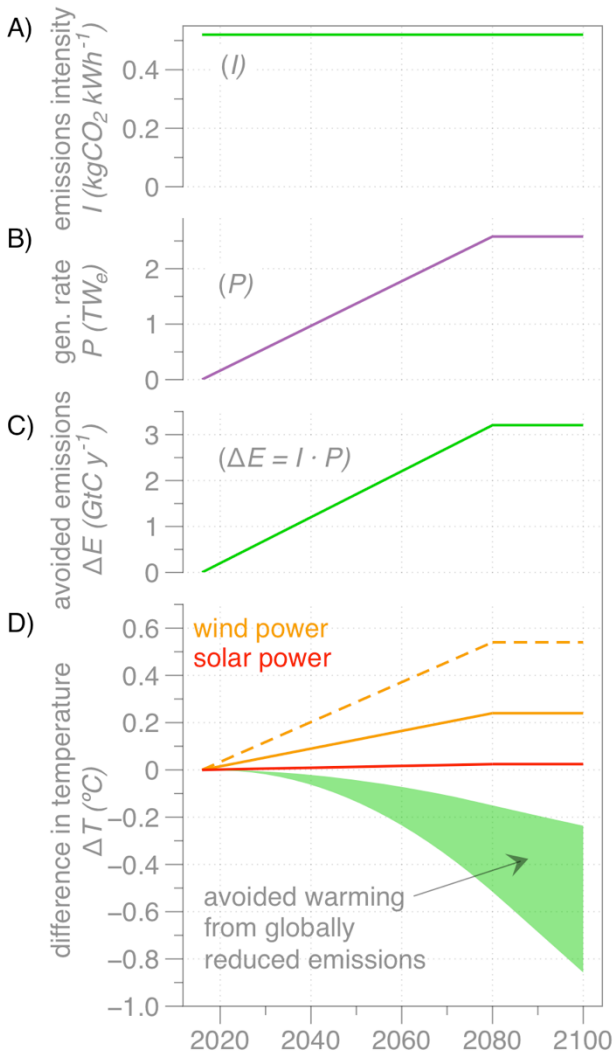

Fig. S8

Companion plot to Fig. 4 of the main text. Climate warming impacts compared to climate benefits of reduced emissions. (**A**) Static global emissions intensity, reflecting the present-day. (**B**) A scenario in which power output, P, from a zero-emissions renewable increases to 2.6 TW_e by 2080 and is constant thereafter. (**C**) Avoided emissions computed as $\Delta E = I \times P$, and (**D**) the resulting 2-meter temperature differences within the wind farm region (dotted lines) and the Continental US (solid lines). Values for wind power linearly scaled from the 0.46 TW_e *benchmark scenario* of the main text, while values for solar are derived from[18]. The green area shows the avoided Continental US warming if all global electricity emissions were zero in 2080, with the range estimated from the min- and max-values within the emissions-to-climate impulse response function.

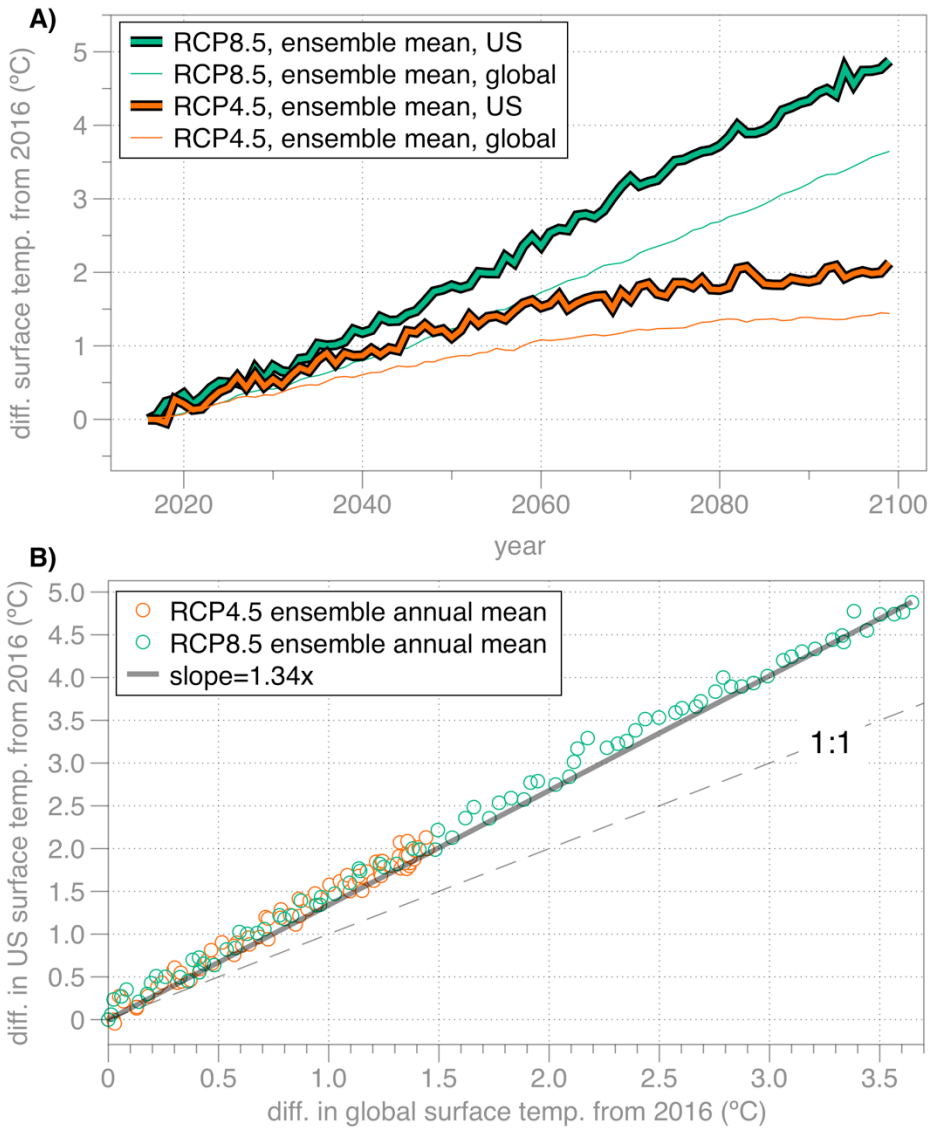

Fig. S9

To estimate the US warming from the global warming estimates from the emissions-to-climate impulse response function, we use the RCP4.5 and RCP8.5 ensemble mean data of Karmalkar et al. (2017); **A)** surface temperature data from 2016 over the Continental US and globally, **B)** using 2016 as the baseline temperature, comparing the difference in global surface temperatures and US surface temperatures. We used the statistical relationship in (B) to rescale the estimates of avoided global warming to estimates of avoided US warming in Fig. 5D.

Table S1. 2-meter air temperature response within the 'hole' region during 2014. Values identified as '0.5 MW_i km^{-2}; no hole' correspond to the original model setup and accompanying Fig. 1, while the '0.5 MW_i km^{-2}; hole' correspond to the results shown in the above Figure. Values within parentheses note the temperature difference from the control.

	control	0.5 MW_i km^{-2}; no hole	0.5 MW_i km^{-2}; hole
all	11.63ºC	12.44ºC (+0.81ºC)	12.02ºC (+0.39ºC)
day	16.86 ºC	17.40ºC (+0.54ºC)	17.25ºC (+0.39ºC)
night	6.39 ºC	7.48ºC (+1.09ºC)	6.78ºC (+0.39ºC)

Table S2.

Values used for the comparison in Fig. 3. Specifics of the reference and the analysis period are noted on the left, as well as the simulation data from our benchmark scenario at the Texas location (100.2ºW, 32.3ºN). Average day and night values were calculated for the observations to allow for a comparison to the simulation data (day = solar shortwave down > 1 W m^{-2}; night = solar shortwave down < 1 W m^{-2}).

		December - February						March - May					
		DAY			NIGHT			DAY			NIGHT		
Reference	Analysis Period	avg.	10:30	13:30	avg.	22:30	1:30	avg.	10:30	13:30	avg.	22:30	1:30
Zhou et al., 2013; Table 7 QA1 values, ΔT, ºC	(2009,2010,2011) -(2003,2004,2005)	0.11	0.41	-0.20	0.22	0.16	0.27	-0.11	-0.22	0.01	0.29	0.25	0.32
Zhou et al., 2013; Table 7 QA1 values, ΔT, ºC	2010-2003	0.14	0.68	-0.41	-0.01	0.05	-0.07	0.42	0.23	0.61	0.29	0.30	0.28
Xia et al., 2015; Table 2, ΔT, ºC	(2010,2011,2012,2013,2014)-(2003,2004)	0.18	0.28	0.07	0.26	0.28	0.23	-0.25	-0.39	-0.11	0.40	0.26	0.53
average weighted by obs. years		0.14			0.20			-0.10			0.34		
this study, simulated at TX location (ΔT), ºC	(2012,2013,2014)-(2012,2013,2014)	0.48			0.65			0.22			0.60		
this study simulated at TX location, control, ºC	2012,2013,2014	10.30			5.41			22.87			14.58		
this study, simulated at TX location, 0.5 MW/km^2, ºC	2012,2013,2014	10.78			6.05			23.08			15.18		
		June - August						September - November					
		DAY			NIGHT			DAY			NIGHT		
Reference	Analysis Period	avg.	10:30	13:30	avg.	22:30	1:30	avg.	10:30	13:30	avg.	22:30	1:30
Zhou et al., 2013; Table 7 QA1 values, ΔT, ºC	(2009,2010,2011) -(2003,2004,2005)	0.17	-0.18	0.52	0.35	0.46	0.24	-0.04	-0.03	-0.04	0.40	0.43	0.37
Zhou et al., 2013; Table 7 QA1 values, ΔT, ºC	2010-2003	1.52	0.84	2.20	0.67	0.70	0.64	0.12	0.18	0.05	0.47	0.59	0.35
Xia et al., 2015; Table 2, ΔT, ºC	(2010,2011,2012,2013,2014)-(2003,2004)	-0.26	-0.38	-0.13	0.42	0.38	0.45	-0.02	0.05	-0.08	0.27	0.37	0.17
average weighted by obs. years		0.15			0.42			-0.01			0.35		
this study, simulated at TX location (ΔT), ºC	(2012,2013,2014)-(2012,2013,2014)	0.34			0.86			0.29			0.54		
this study simulated at TX location, control, ºC	2012,2013,2014	35.47			27.89			24.06			16.11		
this study, simulated at TX location, 0.5 MW/km^2, ºC	2012,2013,2014	35.82			28.75			24.35			16.64		
		Annual											
		DAY			NIGHT								
Reference	Analysis Period	avg.	10:30	13:30	avg.	22:30	1:30						
Zhou et al., 2013; Table 7 QA1 values, ΔT, ºC	(2009,2010,2011) -(2003,2004,2005)	-0.04	-0.03	-0.04	0.25	0.28	0.22						
Zhou et al., 2013; Table 7 QA1 values, ΔT, ºC	2010-2003	0.49	0.42	0.56	0.26	0.31	0.20						
Xia et al., 2015; Table 2, ΔT, ºC	(2010,2011,2012,2013,2014)-(2003,2004)	-0.09	-0.11	-0.06	0.33	0.32	0.34						
average weighted by obs. years		0.01			0.29								
this study, simulated at TX location (ΔT), ºC	(2012,2013,2014)-(2012,2013,2014)	0.33			0.66								
this study simulated at TX location, control, ºC	2012,2013,2014	23.17			16.00								
this study, simulated at TX location, 0.5 MW/km^2, ºC	2012,2013,2014	23.51			16.66								